# Raman and x-ray diffraction studies of Ba doped germanium clathrate $Ba_8Ge_{43}$ at high pressures

Hiroyasu Shimizu[a)]
*Department of Materials Science and Technology, Gifu University, 1-1 Yanagido, Gifu 501-1193, Japan and Environmental and Renewable Energy Systems, Graduate School of Engineering, Gifu University, 1-1 Yanagido, Gifu 501-1193, Japan*

Toshiaki Iitaka
*Computational Astrophysics Lab., RIKEN, 2-1 Hirosawa, Wako, Saitama 351-0198, Japan*

Takumi Fukushima
*Environmental and Renewable Energy Systems, Graduate School of Engineering, Gifu University, 1-1 Yanagido, Gifu 501-1193, Japan*

Tetsuji Kume
*Department of Materials Science and Technology, Gifu University, 1-1 Yanagido, Gifu 501-1193, Japan*

Shigeo Sasaki
*Department of Materials Science and Technology, Gifu University, 1-1 Yanagido, Gifu 501-1193, Japan and Environmental and Renewable Energy Systems, Graduate School of Engineering, Gifu University, 1-1 Yanagido, Gifu 501-1193, Japan*

Nagayoshi Sata
*Institute for Research on Earth Evolution, Japan Agency for Marine-Earth Science and Technology, Yokosuka, Kanagawa 237-0061, Japan*

Yasuo Ohishi
*Japan Synchrotron Radiation Research Institute, Mikazuki-cho, Hyogo 679-5198, Japan*

Hiroshi Fukuoka and Shoji Yamanaka
*Department of Applied Chemistry, Graduate School of Engineering, Hiroshima University, Higashi-Hiroshima 739-8527, Japan*

(Received 4 January 2007; accepted 20 January 2007; published online 30 March 2007)

High-pressure Raman and x-ray diffraxtion (XRD) measurements of a defect clathrate $Ba_8Ge_{43}\square_3$ have been carried out at room temperature up to 40 GPa. Three vibrational modes associated with guest Ba atoms were observed in the low-frequency region, and the structureless spectrum due to Ge vacancies was found in the framework vibrational region. The Raman spectra shows a pressure-induced phase transition at 8 GPa, which is due to the structural distortion through the three-bonded Ge atoms and to the change in the guest-host electronic interaction. Both Raman spectra and XRD patterns present the evidence for the amorphization of $Ba_8Ge_{43}$ around 30–40 GPa. The isostructural phase transition often present in intercalated silicon clathrates and associated with a large volume reduction was not observed for $Ba_8Ge_{43}$ up to 40 GPa. The pressure dependence of the lattice constant $(a)$ normalized by $a_0$ at 1 bar $(a/a_0)$ shows the continuous decrease with pressure until amorphization. From the good coincidence of this curve between $Ba_8Ge_{43}$ and $Ba_8Si_{46}$ at pressures above 15 GPa, we propose that the isostructural phase transition found for $Ba_8Si_{46}$ at 15 GPa may be originated from a defect-induced transformation to $Ba_8Si_{43}\square_3$ with the help of their theoretical equation of state by the first-principles calculations. © *2007 American Institute of Physics*. [DOI: 10.1063/1.2713354]

## I. INTRODUCTION

Group-IV clathrates are open-structured Si, Ge, and Sn cagelike compounds, which have received considerable attention over the past few years.[1,2] In these clathrates with nanoscale cages forming 3D (three-dimensional) networks, alkali and alkaline-earth guest atoms are encapsulated in the cages of the host framework which is formed by tetrahedrally bonded group-IV atoms comprised of two or three different polyhedra.[3] An exciting property of clathrate compounds is that they provide an opportunity to systematically alter material-properties by changing the guest atoms or by replacing some of the framework atoms with metallic species. In these clathrates, the electron-phonon and electron-electron couplings between the guest and the host are key points to understand their characteristic properties such as superconductivity,[4–9] wide band-gap,[10,11] high thermoelectric power [due to the behavior of phonon-glass and electron-crystal (PGEC)],[12,13] and pressure stability.[3,14] These couplings can be explored in part by the study of high-pressure Raman scattering through their vibrational properties of both

[a)]Author to whom correspondence should be addressed. Electronic mail: shimizu@gifu-u.ac.jp

 

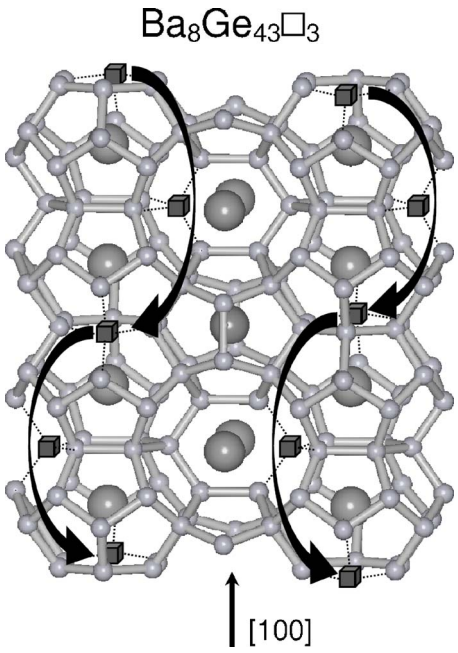


FIG. 1. Crystal structure of type-I $Ba_8Ge_{43}\square_3$ clathrate. There are large and small Ge cages containing the guest Ba atoms. Solid cubes at the 6*c* sites indicate the missing atoms showing the spiral substructure of the Ge vacancies along the <100> direction (Refs. 21–23).

guest atoms inside the cages and the host framework,[15–18] and by the x-ray diffraction (XRD) experiment through their structural properties of the host framework and the position of guest atoms in the cages under high pressures.[3,19,20]

$Ba_8Ge_{43}$ is characterized as a defect clathrate of type-I structure with three missing Ge atoms in the covalent Ge framework, where the vacancies (□) of $Ba_8Ge_{43}\square_3$ (space group $Ia\bar{3}d$, $a$=21.3 Å) show a full ordering. This ordered crystal structure can be considered as a derivative of an "ideal" $Ba_8Ge_{46}$ clathrate type-I structure ($Pm\bar{3}n$, $a'=a/2$) in which three Ge vacancies (per formula unit) are allowed to order in a cubic superstructure with a doubled unit cell parameter (□ at the 24*c* site of space group $Ia\bar{3}d$, which corresponds to half the 6*c* sites in the usual parent type-I clathrate). In the resulting Ge framework, each vacancy is surrounded by four three-bonded Ge species and arranged around $4_1$ fourfold screw axes to form chiral helices along the <100> direction as shown in Fig. 1.[21–23]

The interesting properties of type-I silicon clathrates are three pressure-induced phase transitions,[3] which were studied by Raman scattering[15–18] and XRD experiments,[3,19,20] and theoretical calculations.[19,24] The first transition at 6 to 7 GPa is caused by the displacement of the guest atoms in the large $Si_{24}$ cages. The second transition observed at the pressure range of 15–35 GPa is characterized by a large reduction of cell volume. The mechanism of the isostructural phase transition is not still understood and remains unclear.[3,19,20] The last transition at a pressure range above 32 GPa is an irreversible amorphization.[3,18–20]

In this paper, we present the high-pressure Raman and XRD experiments of $Ba_8Ge_{43}\square_3$ in order to study characteristic properties of the defect germanium clathrate at room temperature up to 40 GPa, and to investigate the mechanism of isostructural phase transition observed in type-I silicon clathrates. Raman spectrum of $Ba_8Ge_{43}$ at 1 bar is different from that expected for an ideal $Ba_8Ge_{46}$ by considering the Raman spectra of $Ba_8Si_{46}$,[15] $Sr_8Ga_{16}Ge_{30}$,[25] and $Ba_8Ga_{16}Ge_{30}$ clathrates[26]; the structureless spectra due to Ge vacancies were observed in the framework vibrational region. The isostructural phase transition with the large volume reduction was not observed for $Ba_8Ge_{43}$ at pressures up to 40 GPa. By comparing the pressure dependence of the lattice constant of $Ba_8Ge_{43}$ with those of typical $Ba_8Si_{46}$ and with the calculated cell volumes of a "virtual" $Ba_8Si_{43}\square_3$ having three Si defects, we propose one model to the mechanism of the isostructural phase transition generally observed in type-I silicon clathrates. The pressure dependence of bulk moduli for $Ba_8Ge_{43}$, $Ba_8Si_{46}$, $Ba_8Si_{43}$, cubic-diamond Si ($d-$Si), and $d-$Ge are investigated in connection with the isostructural phase transition.

## II. EXPERIMENTAL

$Ba_8Ge_{43}$ samples were prepared using an arc furnace; germanium (Katayama Chemical 99.999%), and barium (Katayama Chemical 99%) were mixed in an atomic ratio of 8:43, and arc-melted under argon atmosphere.[21] High-pressure experiments were carried out by using a diamond anvil cell (DAC) with a metal gasket.

The hole of the tungsten-metal gasket serving as the sample chamber was set to about 100 $\mu$m in diameter and 50 $\mu$m in thickness. A single-phase sample of 40 $\mu$m in size was placed into the chamber of the DAC and loaded with a ruby chip for pressure measurements. For fine Raman measurements of $Ba_8Ge_{43}$ which shows very weak Raman signals, we used the dense argon as the pressure-transmitting medium that is free from Raman signals.[15–18,25–27] Raman spectra were measured with a triple polychromator and a charge-coupled device (CCD) detector. The 532 nm line of a solid laser (Coherent Verdi2W) with its intensities of less than 10 mW was used for the excitation. The resolution of the Raman spectra was about 1 $cm^{-1}$.

To make the powder XRD measurements, the synthesized $Ba_8Ge_{43}$ was ground to fine powder, and the powder was pressed into a small pellet by the diamond anvils prior to the setting of the gasket. The small $Ba_8Ge_{43}$ pellet and a ruby chip were then placed into the sample chamber and prepared in the same manner as that for Raman measurements. The pressure media used for the XRD experiments were dense argon and helium. Synchrotron powder XRD measurements were carried out with an imaging plate detector installed at the BL10XU beam line of the SPring-8. The wavelength of the incident x-ray used was 0.041 36 nm. Typical exposure times were 10 min.

## III. RESULTS AND DISCUSSION

### A. Raman scattering at ambient pressure and temperature

Figure 2 shows a Raman spectrum of $Ba_8Ge_{43}$ at ambient pressure and temperature, and those of germanium- and silicon-clathrates for comparison. The Raman frequency for $Ba_8Si_{46}$ at the top of Fig. 2(b) was scaled by the square root

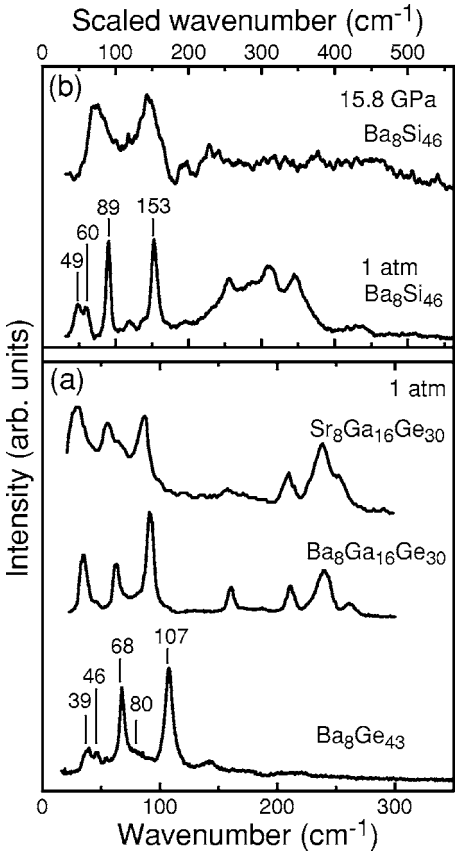


FIG. 2. (a) Raman spectra of the defect clathrate $Ba_8Ge_{43}$, ternary clathrates $Ba_8Ga_{16}Ge_{30}$ (Ref. 26) and $Sr_8Ga_{16}Ge_{30}$ (Ref. 25) at 1 bar, and (b) the $Ba_8Si_{46}$ (Ref. 15) at 1 bar and $p=15.8$ GPa. The numbering of the peaks on the $Ba_8Ge_{43}$ and $Ba_8Si_{46}$ spectra indicate Raman peak wavenumbers. The Raman frequency at the top of $Ba_8Si_{46}$ is scaled by the square root of atomic mass ratio of Si to Ge, 1/1.61.

of an atomic mass ratio of Si to Ge, $(M_{Si}/M_{Ge})^{1/2}=(28.1/72.6)^{1/2}=1/1.61$. The $Ba_8Ge_{43}$ ambient spectrum is different from another clathrate, i.e., the structureless feature (weak Raman scattering intensity) in the framework vibration around 150–300 $cm^{-1}$. On the contrary, the spectral shape of $Ba_8Ge_{43}$ at the low-frequency below 150 $cm^{-1}$ is found to be very similar to that of $Ba_8Si_{46}$ below 200 $cm^{-1}$ at ambient pressure. Three low-frequency peaks of $Ba_8Ge_{43}$ (39, 46, and 68 $cm^{-1}$) can be assigned to the vibrational modes originating from the motion of guest Ba atoms.[15,18] Here, the space group $Ia\bar{3}d$ of $Ba_8Ge_{43}$ predicts nine Raman-active modes of Ba related vibrations; $2A_{1g}+3E_g+4T_{2g}$. However, we cannot unambiguously make the mode assignments because of relatively broad bands containing more than one Raman mode. Furthermore, $Ba_8Ge_{43}$ specimen is not a single crystal, therefore, we cannot make the symmetry-specific polarization measurement at present. For $Ba_8Si_{46}$ the low-frequency peaks at 49, 60, and 89 $cm^{-1}$ had been assigned to the vibrations associated mainly with the guest Ba atoms inside the host Si cages.[15,18,24] The theoretical investigations[24] suggested that their Raman modes are possibly mixed with Si lattice vibrations. Therefore, the same situations will be expected for the $Ba_8Ge_{43}$ spectra. For ternary compounds of $Sr_8Ga_{16}Ge_{30}$[25] and $Ba_8Ga_{16}Ge_{30}$,[26] we can confirm, below 75 $cm^{-1}$, the rattling vibrations assigned to the motion of guest Sr and Ba atoms, respectively.

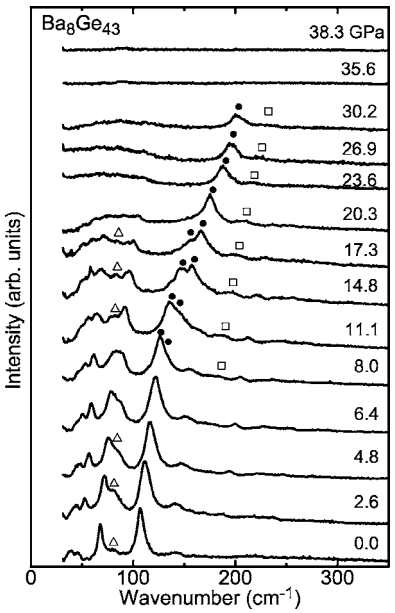


FIG. 3. Raman spectra of $Ba_8Ge_{43}$ at various pressures up to 38.3 GPa and room temperature. Solid circles and open squares indicate new signals appeared through the phase transition at 8 GPa. Open triangles show the softening mode with pressure. Around 30–40 GPa, $Ba_8Ge_{43}$ becomes gradually amorphous.

As reported for Si clathrates,[3,15–18] we know the lowest frequency framework vibration showing the softening with pressure, which is the benchmark of the Si clathrates and also of cubic-diamond Si,[28] having tetrahedral bonds. A peak at 153 $cm^{-1}$ of $Ba_8Si_{46}$ in Fig. 2(b) was assigned to this framework mode. From the similar spectra of $Ba_8Ge_{43}$ and $Ba_8Si_{46}$ at the low-frequency region, we expect a strong peak at 107 $cm^{-1}$ of $Ba_8Ge_{43}$ to be this softening mode. However, this framework vibration did not show the softening with pressure as shown later. A weak signal at 80 $cm^{-1}$ of $Ba_8Ge_{43}$ turned out to be the case of this softening mode. These observations of two Raman modes at 107 and 80 $cm^{-1}$ are consistent with the theoretical calculation[29] of Raman spectra (frequency and intensity) for the ideal type-I $Ge_{46}$ clathrate without guest atoms; intense peak at 89 $cm^{-1}$ ($T_{2g}$) and medium peak at 67 $cm^{-1}$ ($E_g$). It should be noted from Fig. 2(a) that $Ba_8Ge_{43}$ shows very weak Raman signals at a high-frequency vibrational region above 150 $cm^{-1}$, contrary to the Raman spectra of vacancyless $Sr_8Ga_{16}Ge_{30}$[25] and $Ba_8Ga_{16}Ge_{30}$,[26] and the theoretical calculation of $Ge_{46}$.[29] Therefore, the structureless feature of the Raman spectra is due to the three Ge vacancies (□) in $Ba_8Ge_{43}\square_3$. It is noted that our previous result of $Ba_8Si_{46}$[15] at $p=15.8$ GPa in Fig. 2(b) also showed the structureless spectrum in the framework vibrational region. This similarity is investigated in Sec. III D.

### B. Raman scattering at high pressures

Raman spectra of $Ba_8Ge_{43}$ at various pressures up to 38 GPa are shown in Fig. 3. We can find the remarkable spectral changes; the appearance of new Raman bands around 130–180 $cm^{-1}$ at 8 GPa and the disappearance of Raman bands around 30–38 GPa. By analyzing overlapped

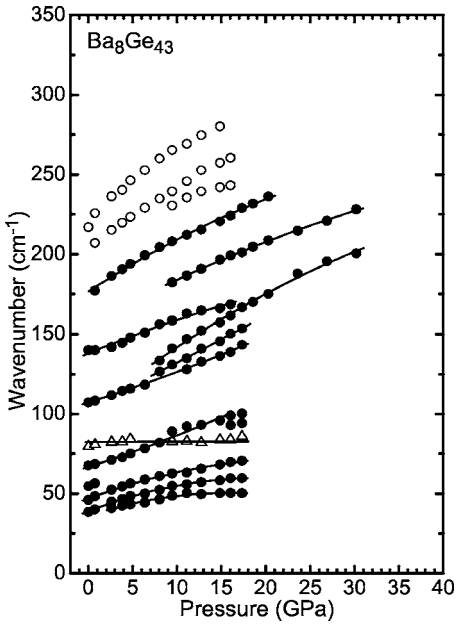


FIG. 4. Pressure dependence of Raman frequency shifts of $Ba_8Ge_{43}$ at room temperature. Open circles show the weak Raman peaks, and open triangles indicate the softening mode. A pressure-induced phase transition exists at about 8 GPa, and the amorphization gradually occurs around 30–40 GPa.

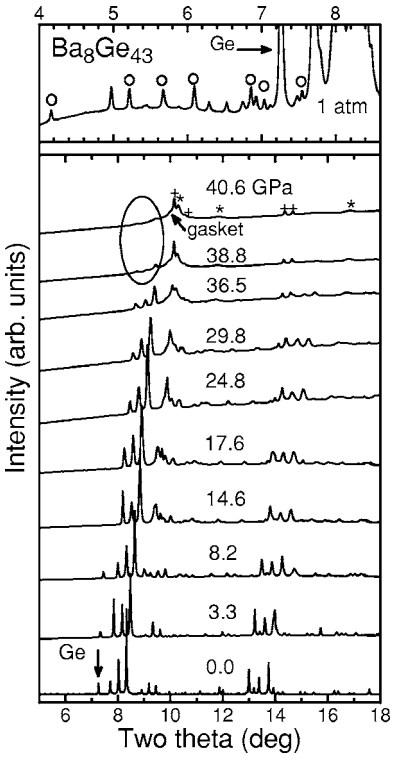


FIG. 5. Observed diffraction patterns of $Ba_8Ge_{43}$ in the $2\theta$ range from 4° to 18° at high pressures up to 41 GPa, where the data up to 17.6 GPa were taken for the first sample, and the data above 17.6 GPa for the second sample. An inset is the enlargement of the lower diffraction angles at 1 bar. Weak peaks indicated by open circles in the inset are corresponding to the superlattice reflections (Ref. 23), which are due to the ordered arrangement of Ge vacancies. An arrow indicates the diffraction peak from the diamond phase of Ge in the minority phase. The XRD patterns of the sample gradually disappeared at pressures around 30–40 GPa and it was completed near 40 GPa as indicated by the marking, and there remain signals from the metal gasket, pressure-transmitting Ar (*), and high pressure $\beta$-Sn phase of Ge (+).

spectra, we can plot the pressure dependence of the Raman frequency as shown in Fig. 4. The soft mode of $Ba_8Ge_{43}$ can be seen around 80 $cm^{-1}$ (see open triangles in Figs. 3 and 4), which was described in the previous section. The weak pressure dependence of the soft-mode frequency may be because the peak frequency is affected by the anti-crossing due to the mode-resonance between 80 $cm^{-1}$ soft mode and 68 $cm^{-1}$ vibrational peak. This softening is similar to the case of Si clathrates and $d-$Si, and is concerned with the softening of TA ($X$) mode observed for $d-$Ge.[30–32]

Next, we investigate the pressure-induced phase transition. It is found that two new peaks grow up at about 8 GPa as indicated by solid circles in Fig. 3. At the same time, a new band appeared at about 180 $cm^{-1}$ as shown by open squares in Fig. 3. These spectral changes suggest the occurrence of the phase transition. As seen in the next section, XRD experiments show no structural change around this pressure range. Therefore, by considering the defect of the $Ba_8Ge_{43}\square_3$ clathrate where there are three-bonded Ge atoms, the appearance of the new peaks may be due to some localized and random strains, i.e., structural distortions. This effect cannot be detected by XRD. A similar Raman spectral change was observed at the same pressure range for $Ba_{24}Si_{100}$,[18] which also comprises of 32% three-bonded Si atoms. Moreover, another additional interpretation of the Raman spectral change can be made with a change in the electronic state. By the change in the guest-host interaction, the electronic distribution will be affected, leading to the evolution of the relative intensities in Raman signals.[3,20,24]

At pressures around 30 GPa, Raman bands almost disappeared as seen in Fig. 3. This can be understood as the onset of pressure-induced amorphization in $Ba_8Ge_{43}$. The amorphization occurs gradually and partially around 30–40 GPa and it is completed at about 40 GPa. This feature is strongly supported by the present XRD study described in the next section. This value of 30–40 GPa is comparable with the amorphization pressure of 40–49 GPa for $Ba_8Si_{46}$.[3,20]

### C. X-ray diffraction at high pressures

Figure 5 shows the observed diffraction patterns of $Ba_8Ge_{43}$ in the $2\theta$ range from 4° to 18° at high pressures up to 41 GPa, where the data up to 17.6 GPa were taken for the first sample, and the data above 17.6 GPa for the second sample. These data were obtained with the argon pressure medium. The experiments using a helium pressure medium have been carried out for the third sample up to 16 GPa, but there is no significant difference in between the results in the cases of Ar and He pressure media. An inset in the figure is the enlargement of the lower diffraction angles at 1 bar. An arrow indicates the diffraction peak from Ge in the minority phase. This XRD pattern of $Ba_8Ge_{43}$ at atmospheric pressure is very close to the recent result by Okamoto *et al.*[23] Weak peaks indicated by open circles in the inset are corresponding to the superlattice reflections,[23] which are due to the ordered arrangement of Ge vacancies, i.e., the doubled unit cell parameter of the usual type-I clathrate. Although these super-

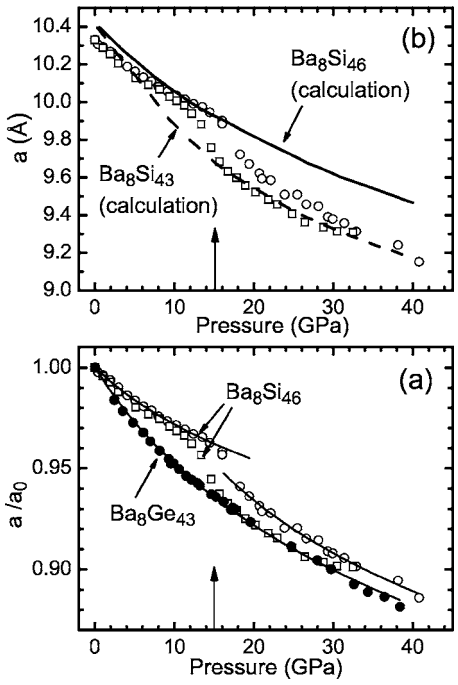


FIG. 6. (a) Pressure dependence of the normalized lattice constant ($a/a_0$) for $Ba_8Si_{46}$ as indicated by open squares and open circles (Refs. 14 and 20) and for the present experimental $Ba_8Ge_{43}$ by solid circles. Solid lines represent the fitted curves by using the Murnaghan's equation of state. (b) Pressure dependence of the experimental lattice constant for $Ba_8Si_{46}$ as shown by open squares and open circles (Refs. 14 and 20), and of the theoretical lattice constants for $Ba_8Si_{46}$ and $Ba_8Si_{43}\square_3$ by the first-principles calculations. Vertical arrows indicate the isostructural phase transition point (=15 GPa) in $Ba_8Si_{46}$.

lattice reflections were observed under high pressures at lower angles, we cannot make more investigations because of their weak reflection signals. The intensity change in XRD lines with pressure can be seen somewhere in Fig. 5, but they are not showing the systematic and exact diffraction intensities, because the obtained diffraction rings for the sample were spotty. It is difficult to discuss the evolution of atomic positions using the intensity changes.

From high-pressure data, we obtained the pressure dependence of lattice constant ($a$). Figure 6(a) shows $a/a_0$ normalized by the lattice constant $a_0$ at 1 bar. This normalized lattice constant of $Ba_8Ge_{43}$ decreases continuously with increasing pressure up to 40 GPa (see solid circles). Therefore, there exists no isostructural phase transition associated with the dramatic volume reduction, in contrast to the case of $Ba_8Si_{46}$ as shown by open squares and open circles in Fig. 6(a).[14,20] Here, solid lines in Fig. 6(a) represent the fitted curves by using the Murnaghan's equation of state (EOS).[33] It is surprising that the normalized lattice constants of $Ba_8Si_{46}$ above 15 GPa, i.e., above the isostructural phase transition, show almost close values as those of $Ba_8Ge_{43}$. This remarkable behavior is investigated in the next section.

In Fig. 5 we can see that the XRD patterns of the sample gradually disappeared at pressures around 30–40 GPa and it was completed near 40 GPa as indicated by marking, and there remain only signals from the metal gasket, pressure-transmitting Ar (marked with *),[34] and high pressure $\beta$-Sn phase of the minority Ge (marked with +).[35] The weak signals from the $\beta$-Sn phase of Ge are kept constant in intensity and independent of the disappearance of XRD peaks of $Ba_8Ge_{43}$. Therefore, the disappearance of XRD patterns evidences the amorphization of $Ba_8Ge_{43}$ around 30–40 GPa, which is consistent with the result of a high-pressure Raman study mentioned in the previous section. It is noted that this value of 30–40 GPa is comparable with 40–49 GPa of $Ba_8Si_{46}$ determined by the XRD study.[20]

### D. Isostructural phase transition of type-I clathrates: Experimental and theoretical EOS, and bulk modulus at high pressures

The isostructural phase transition characterized by an important volume collapse without the structural change was observed for $Ba_8Si_{46}$, $K_8Si_{46}$, and $I_8Si_{44}I_2$.[3,14,19,20] For $Ba_8Si_{46}$ San-Miguel *et al.*[20] discussed its physical origin by the change in electronic hybridization between Ba atoms and the Si small cages. However, it is not conclusive, because they only observed minor changes on the electronic structure during the phase transition, using XRD and x-ray absorption spectroscopy.[20] Here, we propose another possible mechanism for its phase transition from XRD and Raman results, and by the theoretical calculations of EOS for $Ba_8Si_{46}$ and $Ba_8Si_{43}$.

In Fig. 6(a) we confirmed that the pressure dependence of $a/a_0$ for $Ba_8Ge_{43}$ shows almost the close value as that of $Ba_8Si_{46}$ at pressures after the isostructural phase transition. This experimental result strongly indicates that $Ba_8Si_{46}$ may transform to $Ba_8Si_{43}\square_3$, producing three Si vacancies at 15 GPa, even though the guest-host interactions are subtly different between Si- and Ge-clathrates. Therefore, we calculated the pressure dependence of the lattice constant ($a$), i.e., the EOS for $Ba_8Si_{46}$ and $Ba_8Si_{43}$ by using the first-principles electronic state code, CASTEP 4.2 based on the plane-wave basis set,[36] the Vanderbilt-type ultrasoft pseudopotentials[37] for electron-ion interaction, and GGA-PBE for exchange-correlation interaction.[38] The cut-off energy was set to 160 eV and the Brillouin zones were sampled with $2\times2\times2$ $k$-points. For $Ba_8Si_{43}$, the partially occupied Si ($6c$) sites with random configurations were further modeled by the ordered unit cell where six $6c$ sites are occupied by three Si atoms with maximum symmetry. As the result, the unit cell for $Ba_8Si_{43}$ becomes trigonal with an $R32$ symmetry. After geometric optimization, however, it was found that the unit cell is close to the original $Pm\bar{3}n$ symmetry and may approximate random occupation very well. As seen in Fig. 6(b), the calculated lines of lattice constants as a function of pressure for $Ba_8Si_{46}$ and $Ba_8Si_{43}$ show good agreement with experimental values[14,20] before and after the isostructural phase transition, respectively. Therefore, we propose the important effect of three Si vacancies on the isostructural phase transition at 15 GPa. Since this transition is reversible,[15] the lost Si atoms may be existing near its lattice points due to the slow diffusion of Si atoms. As for the case of $Ba_8Ge_{43}$, showing no isostructural phase transition up to the amorphization pressure of 40 GPa, we can imagine that the ideal $Ba_8Ge_{46}$ had already made the isostructural phase transition to

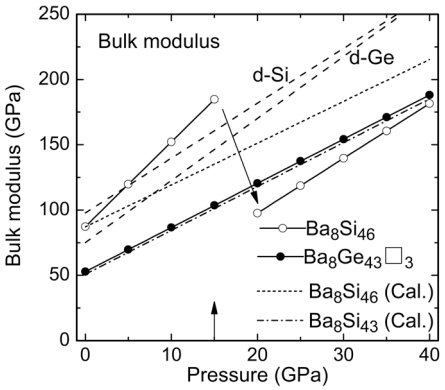


FIG. 7. Pressure dependence of bulk moduli of $Ba_8Ge_{43}$, $Ba_8Si_{46}$ (experiment and calculation), $Ba_8Si_{43}$ (calculation), cubic-diamond Si ($d-$Si), and $d-$Ge. The vertical arrow indicates the isostructural phase transition point (=15 GPa) in $Ba_8Si_{46}$.

$Ba_8Ge_{43}$ associated with the large volume reduction at negative pressures, by considering a hypothetical phase diagram at both positive and negative pressures.

Moreover, our Raman results also support this model of the defect-induced mechanism. In Fig. 2(b) we can see the remarkable Raman spectral change of $Ba_8Si_{46}$ above 15 GPa, i.e., structureless feature in the framework vibrational region.[15] This spectrum is similar to the structureless spectrum of the defect clathrate $Ba_8Ge_{43}$ at 1 bar in Fig. 2(a).

The bulk modulus is an important property of Si- and Ge-clathrate.[3,14,20] We investigate the pressure dependence of the bulk modulus, $B(p)=B_0+B'_0p$ for $Ba_8Ge_{43}$, $Ba_8Si_{46}$, $Ba_8Si_{43}$, cubic-diamond Si ($d-$Si), and $d-$Ge, where $B_0$ is a value at 1 bar, and $B'_0$ is its pressure derivative. The procedures are as follows; by using experimental $a/a(p_0)$ of $Ba_8Ge_{43}$, $Ba_8Si_{46}$,[20] $d-$Si,[31,39] and $d-$Ge,[31,39] and our calculated $a/a(p_0)$ of $Ba_8Si_{46}$ and $Ba_8Si_{43}$, we fitted them to the following Murnaghan's equation of state:[31]

$$\frac{a}{a(p_0)} = \left[\frac{B_0 + B'_0 p}{B_0 + B'_0 p_0}\right]^{-1/(3B'_0)}, \quad (1)$$

where $a(p_0)$ is a lattice constant at pressure $p_0$. By using fitted parameters of $B_0$ and $B'_0$, the bulk moduli $B(p)(=B_0+B'_0p)$ are presented against pressure in Fig. 7: For the present $Ba_8Ge_{43}$, $B_0=52.8$ GPa, and $B'_0=3.4$ were estimated, which are comparable with theoretical values of $B_0=61.3$ GPa and $B'_0=4.8$ for the ideal type-I $Ge_{46}$ clathrate without guest atoms.[29] Although $d-$Si and $d-$Ge show the phase transition at pressures around 11 GPa, their $B$ are extrapolated linearly to higher pressures for comparison with Si- and Ge-clathrates. It is emphasized that the $B$ of $Ba_8Si_{46}$ shows the abrupt change to the lower value at a pressure of approximately 15 GPa, which become close to the values of the defect clathrates $Ba_8Ge_{43}$ and the virtual $Ba_8Si_{43}$. This change of the pressure dependence of bulk moduli for their clathrates also supports our model proposed for the mechanism of the isostructural phase transition generally observed in type-I silicon clathrates.

## IV. SUMMARY

High-pressure Raman and XRD measurements of the defect clathrate $Ba_8Ge_{43}\square_3$ were carried out at room temperature of up to 40 GPa. Raman studies revealed that (1) three vibrational peaks due to the motion of Ba atoms exist at 39, 46, and 68 $cm^{-1}$, (2) structureless spectrum of $Ba_8Ge_{43}$, due to the Ge vacancies, in the framework vibrational region, which is similar to that of $Ba_8Si_{46}$ at pressures above the isostructural phase transition (=15 GPa), (3) the phase transition at 8 GPa due to the structural distortion and to the change in guest-host electronic interaction, (4) the irreversible amorphization around 30–40 GPa. XRD studies showed that the lattice constant of $Ba_8Ge_{43}$ decreases continuously with pressure up to 40 GPa where the irreversible amorphization occurs completely. There exists no isostructural phase transition associated with the large volume reduction up to 40 GPa, in contrast to some cases in type-I Si clathrates.

We propose the possible mechanism for the isostructural phase transition observed for $Ba_8Si_{46}$ at 15 GPa: It is the defect-induced phase transition associated with the transformation from $Ba_8Si_{46}$ to $Ba_8Si_{43}\square_3$. By considering that the pressure dependence of normalized lattice constants $(a/a_0)$ of $Ba_8Ge_{43}$ is a good coincident with that of $Ba_8Si_{46}$ above 15 GPa, we calculated lattice constants of $Ba_8Si_{46}$ and $Ba_8Si_{43}$, which agree surprisingly with the experimental values[3,14,20] before and after the isostructural phase transition of $Ba_8Si_{46}$, respectively. Furthermore, structureless Raman spectrum of $Ba_8Ge_{43}\square_3$ in the framework vibrational region is similar to that of $Ba_8Si_{46}$ at pressures above 15 GPa, evidencing the possibility of its transformation to $Ba_8Si_{43}\square_3$. At last, the pressure dependence of bulk moduli for $Ba_8Ge_{43}$, $Ba_8Si_{46}$, $Ba_8Si_{43}$, $d-$Si, and $d-$Ge were investigated in connection with the isostructural phase transition.

## ACKNOWLEDGMENTS

The results of the calculations were performed by using the RIKEN Super Combined Cluster (RSCC). This work was partially supported by the KAKENHI (Contract No. 18540315) of the Ministry of Education, Culture, Sports, and Technology of Japan.

[1] J. S. Kasper, P. Hagenmuller, M. Pouchard, and C. Cros, Science **150**, 1713 (1965).
[2] S. Bobev and S. C. Sevov, J. Solid State Chem. **153**, 92 (2000), and references are therein.
[3] A. San Miguel and P. Toulemonde, High Press. Res. **25**, 159 (2005).
[4] H. Kawaji, H. O. Horie, S. Yamanaka, and M. Ishikawa, Phys. Rev. Lett. **74**, 1427 (1995).
[5] S. Yamanaka, E. Enishi, H. Fukuoka, and M. Yasukawa, Inorg. Chem. **39**, 56 (2000).
[6] K. Tanigaki, T. Shimizu, K. M. Itoh, J. Teraoka, Y. Moritomo, and S. Yamanaka, Nat. Mater. **2**, 653 (2003).
[7] D. Connétable, V. Timoshevskii, B. Masenelli, J. Beille, J. Marcus, B. Barbara, A. M. Saitta, G. M. Rignanese, P. Mélinon, S. Yamanaka, and X. Blase, Phys. Rev. Lett. **91**, 247001 (2003).
[8] H. Fukuoka, J. Kiyoto, and S. Yamanaka, J. Phys. Chem. Solids **65**, 333 (2004).
[9] P. Toulemonde, Ch. Adessi, X. Blase, A. San Miguel, and J. L. Tholence, Phys. Rev. B **71**, 094504 (2005).
[10] J. Gryko, P. F. McMillan, R. F. Marzke, G. K. Ramachandran, D. Patton, S. K. Deb, and O. F. Sankey, Phys. Rev. B **62**, R7707 (2000).

[11]D. Connétable, V. Timoshevskii, E. Artacho, and X. Blase, Phys. Rev. Lett. **87**, 206405 (2001).
[12]G. S. Nolas, T. J. R. Weakley, J. L. Cohn, and R. Sharma, Phys. Rev. B **61**, 3845 (2000).
[13]J. S. Tse, K. Uehara, R. Rousseau, A. Ker, C. I. Ratcliffe, M. A. White, and G. Mackay, Phys. Rev. Lett. **85**, 114 (2000).
[14]A. San Miguel, P. Mélinon, D. Connétable, X. Blase, F. Tournus, E. Reny, S. Yamanaka, and J. P. Itié, Phys. Rev. B **65**, 054109 (2002).
[15]T. Kume, H. Fukuoka, T. Koda, S. Sasaki, H. Shimizu, and S. Yamanaka, Phys. Rev. Lett. **90**, 155503 (2003).
[16]T. Kume, T. Koda, S. Sasaki, H. Shimizu, and J. S. Tse, Phys. Rev. B **70**, 052101 (2004).
[17]H. Shimizu, T. Kume, T. Kuroda, S. Sasaki, H. Fukuoka, and S. Yamanaka, Phys. Rev. B **68**, 212102 (2003).
[18]H. Shimizu, T. Kume, T. Kuroda, S. Sasaki, H. Fukuoka, and S. Yamanaka, Phys. Rev. B **71**, 094108 (2005).
[19]J. S. Tse, S. Desgreniers, Z. Q. Li, M. R. Ferguson, and Y. Kawazoe, Phys. Rev. Lett. **89**, 195507 (2002).
[20]A. San Miguel, A. Merlen, P. Toulemonde, T. Kume, S. Le Floch, A. Aouizerat, S. Pascarelli, G. Aquilanti, O. Mathon, T. Le Bihan, P. Itié, and S. Yamanaka, Europhys. Lett. **69**, 556 (2005).
[21]H. Fukuoka, J. Kiyoto, and S. Yamanaka, J. Solid State Chem. **175**, 237 (2003).
[22]W. C. Carrillo-Cabrera, S. Budnyk, Y. Prots, and Y. Grin, Z. Anorg. Allg. Chem. **630**, 2267 (2004).
[23]N. L. Okamoto, K. Tanaka, and H. Inui, Acta Mater. **54**, 173 (2006).
[24]J. S. Tse, T. Iitaka, T. Kume, H. Shimizu, K. Parlinski, H. Fukuoka, and S. Yamanaka, Phys. Rev. B **72**, 155441 (2005).
[25]G. S. Nolas and C. A. Kendziora, Phys. Rev. B **62**, 7157 (2000).
[26]Y. Takasu, T. Hasegawa, N. Ogita, M. Udagawa, M. A. Avila, and T. Takabatake, Physica B (Amsterdam) **383**, 134 (2006); Phys. Rev. B **74**, 174303 (2006).
[27]H. Shimizu, H. Tashiro, T. Kume, and S. Sasaki, Phys. Rev. Lett. **86**, 4568 (2001).
[28]B. A. Weinstein and G. J. Piermarini, Phys. Rev. B **12**, 1172 (1975).
[29]J. Dong and O. F. Sankey, J. Phys. Condens. Matter **11**, 6129 (1999).
[30]T. Soma, H. Matsuo, and Y. Saitoh, Solid State Commun. **39**, 913 (1981).
[31]D. Olego and M. Cardona, Phys. Rev. B **25**, 1151 (1982).
[32]T. P. Mernagh and L. G. Liu, J. Phys. Chem. Solids **52**, 507 (1991).
[33]F. D. Murnaghan, Proc. Natl. Acad. Sci. U.S.A. **30**, 244 (1944).
[34]L. W. Finger, R. M. Hazen, G. Zou, H. K. Mao, and P. M. Bell, Appl. Phys. Lett. **39**, 892 (1981).
[35]R. J. Nelmes, H. Liu, S. A. Belmonte, J. S. Laveday, M. I. McMahon, D. R. Allan, D. Hausermann, and M. Hanfland, Phys. Rev. B **53**, R2907 (1996).
[36]M. C. Payne, M. P. Teter, D. C. Allan, T. A. Arias, and J. D. Joannopoulos, Rev. Mod. Phys. **64**, 1045 (1992).
[37]D. Vanderbilt, Phys. Rev. B **41**, 7892 (1990).
[38]J. P. Perdew, K. Burke, and M. Ernzerhof, Phys. Rev. Lett. **77**, 3865 (1996).
[39]Z. Sui, H. H. Burke, and I. P. Herman, Phys. Rev. B **48**, 2162 (1993).